# Simulating the RRS James Clark Ross as Part of a Multiobjective Design Process

Adam Kwiatkowski, Patrick Palmer, Arturo Molina-Cristobal, Richard Bridgeman, Geoff Parks
Engineering Design Centre (EDC), Department of Engineering
University of Cambridge, Cambridge, England
Email: aek33@cam.ac.uk, prp@cam.ac.uk, am664@cam.ac.uk, ribr@bas.ac.uk, gtp10@cam.ac.uk

***Abstract*—A model is developed for the RRS James Clark Ross using the Virtual Test Bed (VTB) simulation package. The model is integrated into a multiobjective optimisation process through a simulation interface developed for this purpose. The interface allows for visualisation of the optimisation results, and facilitates the transfer of design parameters to the simulation model. The simulation model is applied to the existing James Clark Ross design, and the effect of hybridising the propulsion system by adding a battery and IGBT inverter to provide power factor compensation for the DC drive is explored.**

## I. Introduction

This paper presents a simulation model of the James Clark Ross that can be used as part of the development process for a future ship design, or upgrade to the existing design. One possible upgrade for the James Clark Ross is the hybridisation of the propulsion system by adding a battery and IGBT inverter. Hybridising the design in this way has benefits both economically and environmentally, offering both better efficiency and fuel consumption, by avoiding the need to run the diesel engines lightly loaded.

Determining the specification of the design, such as the sizing of the battery and inverter, can be difficult to achieve manually given the large number of components that make up the James Clark Ross and its multi-role use. A more structured approach is to use a multiobjective optimisation to explore possible design parameters, which results in a number of optimal designs. For the optimisation to be carried out in a realistic amount of time, the model used is limited to operation under steady state conditions. Adding the VTB simulation model allows the designer to further characterise the possible designs with regard to their transient behaviour and further performance criteria.

### A. RRS James Clark Ross

The RRS James Clark Ross, shown in Figure 1, is one of two Royal Research Ships (RRS) in current service operated by the British Antarctic Survey (BAS). The ship not only provides logistic support to BAS bases operating in the Antarctic, but is also equipped with some of the most advanced facilities for oceanographic research. The ship is a capable icebreaker, able to achieve a steady 2 knots through level sea ice 1 metre thick. As a research vessel, the power and propulsion system is also required to be ultra quiet to limit interference with equipment, such as the often used underwater hydro-acoustic sensors.

Fig. 1. The RRS James Clark Ross

In order to meet the wide range of ship operating conditions, the power system is supplied by four diesel generators, two 3100kW output and two 1000kW output, that can be used in any combination. Ship propulsion is provided by a single fixed pitch propeller, along with bow and stern thrusters to provide additional manoeuvrability. The main propeller is powered by two DC motors in parallel with a combined rating of 6248kW [1]. The DC motors are fed from the 660V AC bus via a three phase thyristor converter, which provides good efficiency and low noise operation.

A disadvantage of a DC drive is the variable power factor, which varies with the thyristor converter output voltage, and hence the load on the DC motor. A poor power factor can lead to an additional diesel generator set having to be brought online which reduces efficiency and increases the amount of maintenance required. By upgrading the James Clark Ross to a battery hybrid system, the battery and IGBT inverter can act as a power factor compensator by producing reactive power as required.

### B. The Design and Optimisation Process

A large system, such as the RRS James Clark Ross, contains a number of components each with their own measure of performance. Optimising the system for just one of these measures, or *objectives*, will likely result in a number of components having poor performance. Optimising each objective separately is unlikely to yield the best solution due to trade offs between some of the objectives. To obtain a solution that provides the best compromise between the many objectives,

978-1-4244-8218-4/10/$26.00 ©2010 Crown

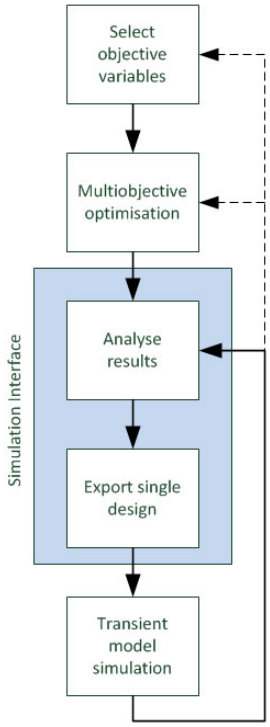


Fig. 2. The Design and Optimisation Process

they all have to be optimised for simultaneously as part of a multiobjective optimisation. Unlike for a single objective optimisation, optimising multiple objectives simultaneously does not usually result in a single solution [2]. Instead a number of possible solutions are obtained that, without further information on the relative importance of the objectives, are considered to be equally valid. The set of solutions is known as a *Pareto Front*.

Due to the computationally expensive nature of multiobjective optimisation, the model used in such a process is unlikely to be particularly detailed, and restricted to analysing the steady state behaviour. A more detailed simulation model, such as that proposed, which examines the transient behaviour of the ship's systems can be used to introduce additional constraints on the design at this stage, narrowing down the number of acceptable solutions. A tool is therefore required that allows the designer to visualise and analyse the optimisation results for the purpose of identifying designs that are worthy of further simulation. In the objective space, the tool will reveal if objectives are in conflict with each other and in addition its shape will provide initial knowledge of how weak or strong a trade-off is. In the decision space, the tool will give some initial information of the sensitivities of the parameters, and will reveal to some degree which ones are "active" and which ones have little impact on the performance [3]. The tool should additionally facilitate a smooth progression between the optimisation and VTB simulation model, by providing an interface that allows easy insertion of design solution parameters into the VTB model.

Such a design process is shown in Figure 2. In the case of a battery hybrid design, the optimisation would attempt to optimise for the size of the battery and inverter for maximum efficiency, under the assumption that when required to by the operating conditions, the battery and inverter system would also be able to supply the reactive power to maintain a close to unity power factor. This allows the optimisation to calculate the performance of the design assuming that the diesel engines only need to meet the real power requirements. This can then be compared to the existing design to identify the potential economic savings.

The optimisation would not however, be able to size the battery for the transient operation when performing power factor compensation as no battery power is necessary for purely reactive power compensation. Other factors such as heat dissipation and the type of battery to be used can also be examined using the VTB model to ensure that the design is suitable.

## II. Simulation Interface

The aim of the interface is to facilitate the smooth transfer from the output of an optimisation to the VTB simulation. Whilst a multi-objective optimisation will provide a number of possible designs, the VTB simulation is only able to simulate one design at a time. Therefore part of the job of the interface is provide features that aid the user in selecting designs that may require further simulation.

The simulation interface is shown in Figure 3. The program is written in MATLAB, and loads optimisation results contained in a MATLAB .mat file. The program provides three plots to allow the designer to explore the output of the optimisation. The design and objective variable plots allow the user to display any combination of two or three of their respective variables, where each design is represented by a blue circle, as shown in Figure 3.

The Pareto Front for two objectives is a curve, and for three variables is a surface. The parallel coordinates plot allows the user to plot more than three objective variables at the same time [4]. In this plot each design is represented by a line. Selecting a design from any of the plots, highlights the same design in all three plots at once. The program also displays the relavent design and objective variables that were calculated by the optimisation.

When a design is selected, the user can choose to export the design variables to a VTB file of their choice. When a target VTB file is selected, the program parses the file for all the models it contains, and identifies their parameters. The user is then able to associate design variables with a parameter of their choice. The program then creates a new VTB file where parameters have been assigned their associated design variable values.

## III. Simulation Model

### A. Virtual Test Bed (VTB)

Virtual Test Bed is a simulation package that has been designed for modelling interdisciplinary dynamic systems.

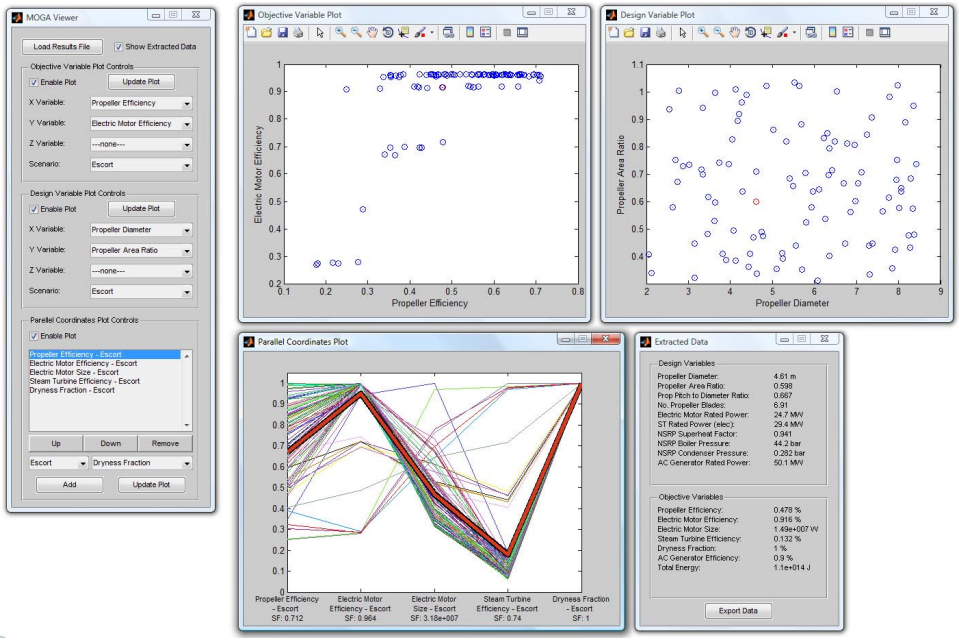


Fig. 3. Simulation interface with a design selected

Whilst the focus of the development has been on the simulation of power systems for navy platforms, the software can simulate a wide range of models and disciplines including electrical, mechanical, thermal and chemical [5].

Models use *natural coupling*, which ensures that any conservation laws such as conservation of energy, are automatically enforced [6]. This is implemented using a Resistive Companion (RC) method, which is a discretised form of the differential equations that describe the model. The ports of the model, termed *natural ports*, have no associated direction and are defined in terms of across and through variables. An electrical component would have voltage as the across variable, and current as the through variable. The Resistive-Companion method requires the form:

$$\mathbf{I} = \mathbf{G} \cdot \mathbf{V} - \mathbf{B} \tag{1}$$

where $\mathbf{I}$ is a vector of through variables, $\mathbf{V}$ is a vector of across variables, $\mathbf{G}$ is a Jacobian Matrix, and $\mathbf{B}$ is a vector that depends on the past history of across and through variables.

Another type of port used by the simulation is the *signal port*. It is associated with the flow of information and has a direction, hence it is either an input or output. It is primarily used for the design and validation of controllers, such as the DC thyristor drive controller, and associated control algorithms. It is also used to pass additional values that are not defined using natural ports, such as temperature for thermodynamic modelling.

### B. Model Implementation

Figure 4 shows the complete simulation model for the battery hybrid propulsion system. The DC motor is driven by a 12 pulse thyristor converter, with control provided by two feedback loops: an inner feedback loop controlling armature current, and an outer loop controlling shaft speed.

*1) DC Motor Model:* The equivalent circuit of the DC motor is shown in Figure 5. The DC motor armature voltage is given by:

$$V_A = R_A I_A + L_A \frac{dI_A}{dt} + \epsilon_A \tag{2}$$

The induced e.m.f. $\epsilon_A$ is related to the flux $\phi$ and angular velocity $\omega$ by:

$$\epsilon_A = k_e \phi \omega \tag{3}$$

The amount of magnetic flux is controlled by the current through the field winding:

$$k_e \phi = k_m L_f I_f(t) \tag{4}$$

where $k_m$ and $k_e$ are constants. The field current and voltage are related by:

$$V_f = R_f I_f + L_f \frac{dI_f}{dt} \tag{5}$$

The induced torque of the DC motor is determined by the armature current and flux:

$$\tau_{ind} = k_T \phi I_A \tag{6}$$

This can be related to the mechanical dynamic behaviour by:

$$\tau_{ind} = k_m L_f I_f(t) I_A = J \frac{d\omega}{dt} + b\omega + \tau_m \tag{7}$$

where $J$ is the shaft inertia, $b$ is a mechanical drag coefficient, and $\tau_m$ is the mechanical torque due to the mechanical load.

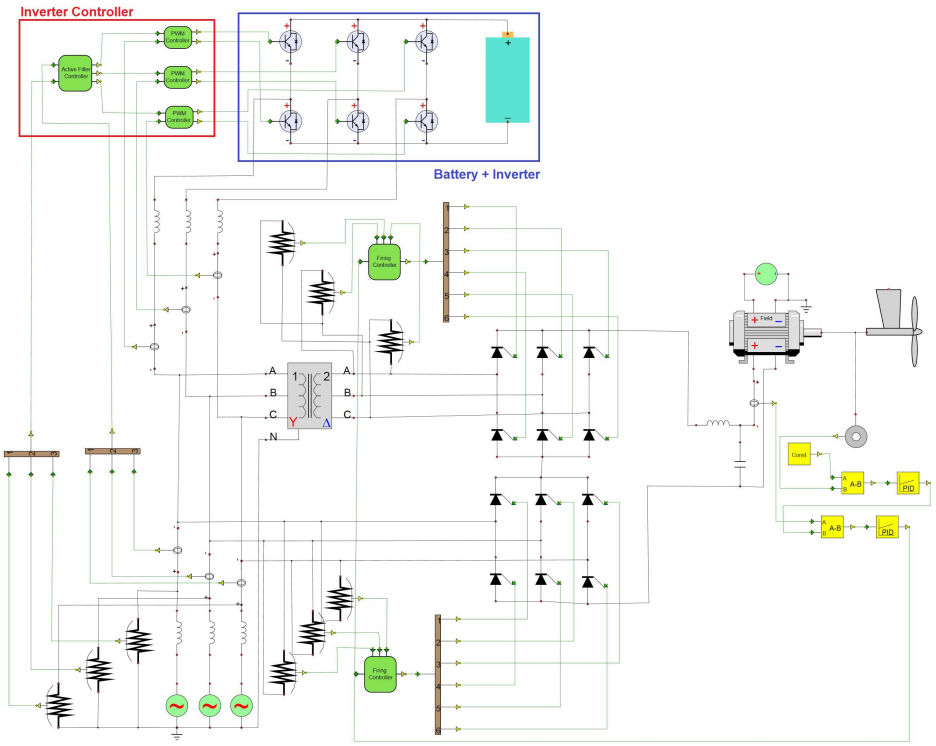


Fig. 4. Battery Hybrid Propulsion System Simulation Model

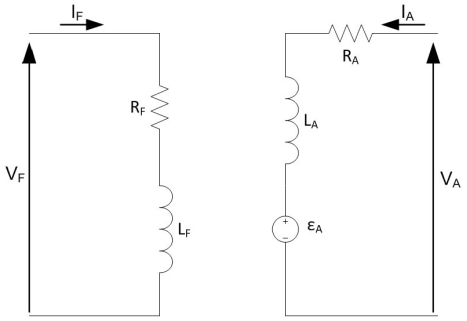


Fig. 5. DC Motor Equivalent Circuit

*2) Inverter Controller:* The inverter and battery act as an active filter to compensate for reactive power and harmonics by injecting compensating currents into the supply. The active filter controller monitors the current and voltage waveforms of the supply, and calculates the instantaneous real and imaginary powers according to the instantaneous p-q theory developed by [7].

The first step in instantaneous p-q theory is to transform the current and voltage waveforms from the *abc* phase domain into the $\alpha\beta 0$ domain by using the Clarke transform [8]. The instantaneous real and imaginary powers are then given by:

$$\begin{bmatrix} p \\ q \end{bmatrix} = \begin{bmatrix} v_\alpha & v_\beta \\ -v_\beta & v_\alpha \end{bmatrix} \begin{bmatrix} i_\alpha \\ i_\beta \end{bmatrix} \tag{8}$$

These can be further divided into average and oscillating components:

$$p = \bar{p} + \tilde{p} \tag{9}$$

$$q = \bar{q} + \tilde{q} \tag{10}$$

The oscillating components have an average value of zero and so overall do not contribute to power transfer, but instead induce harmonics into the supply. The average and oscillating parts can be separated using a low pass filter.

The active filter can now eliminate either harmonics or reactive power by counteracting different combinations of these four terms $\bar{p}, \tilde{p}, \bar{q}$ and $\tilde{q}$. To compensate for reactive power both $\bar{q}$ and $\tilde{q}$ are eliminated. If $\tilde{p}$ is also eliminated, then only constant real power $\bar{p}$ remains. This will therefore additionally eliminate harmonics. After determining which terms are to be compensated for, the inverse Clarke Transform can be used to obtain the compensating currents $i^*_{Ca}$, $i^*_{Cb}$ and $i^*_{Cc}$.

For each phase, a PWM controller compares the output current of the active filter $i_{Ca}$, with the reference current generated by the active filter controller $i^*_{Ca}$. If the reference current is positive, then the upper IGBT of the inverter leg is tuned on when:

$$i_{Ca} < i^*_{Ca} - \epsilon \tag{11}$$

where $\epsilon$ is a constant. It is not turned off until:

$$I_{Ca} > I^*_{Ca} + \epsilon \tag{12}$$

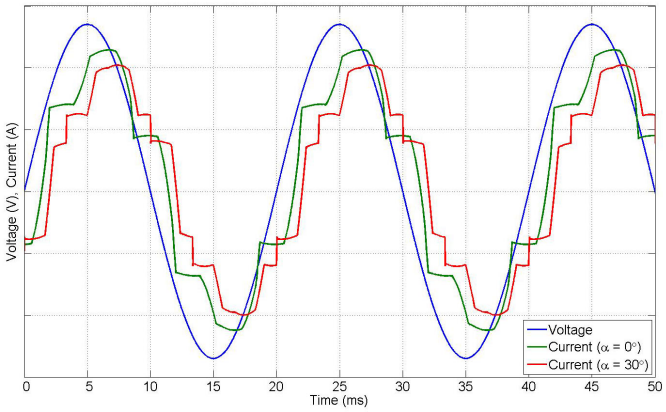


Fig. 6. AC Bus Current and Voltage Waveforms

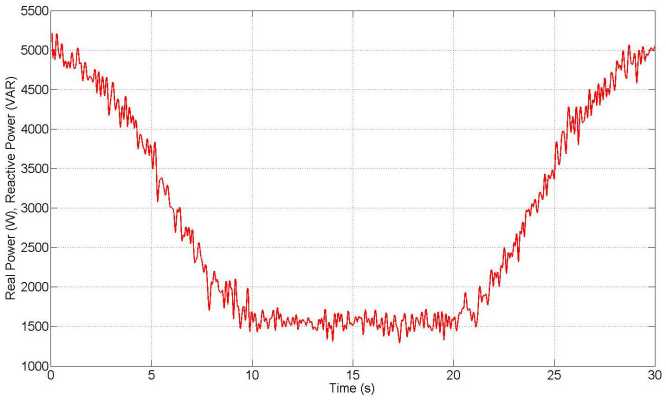


Fig. 7. Real Power Load

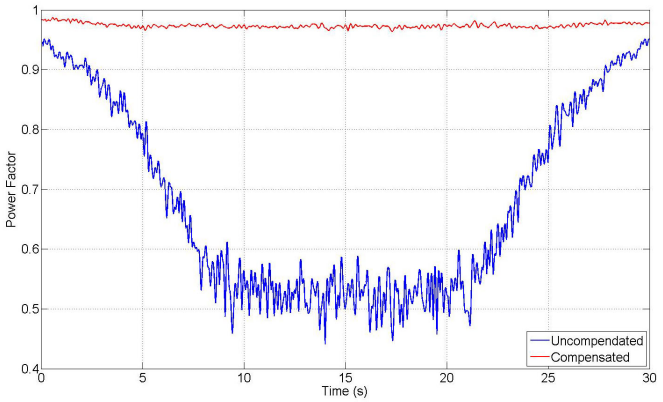


Fig. 8. Power Factor of DC Propulsion Drive

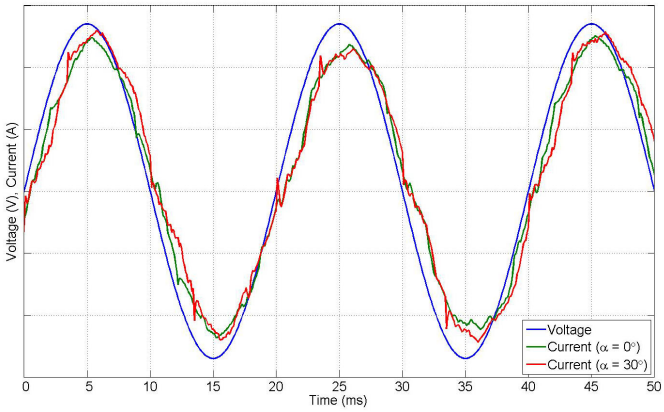


Fig. 9. Supply Current and Voltage with Reactive Power Compensation

Due to the hysteresis, the IGBT cannot turn on again until the condition of equation 11 is met. Hence the output current $i_{Ca}$ will oscillate between the lower and upper bounds on $i^*_{Ca}$ defined by $\epsilon$. The conditions are reversed when $i^*_{Ca}$ is negative, and the lower IGBT is switched instead.

## IV. Results

Figure 6 shows the current and voltage waveforms for a single phase of the AC bus using the DC drive simulation model of Figure 4 but without the active filter operating. It can be seen that an increase in thyristor firing angle $\alpha$ (0-30°), which corresponds to a decrease in DC motor load, causes a further phase shift of the current waveform with respect to voltage, leading to a decrease in power factor.

This is further illustrated by applying a basic DC motor loading scenario where the DC motor load is varied as shown in Figure 7. Figure 8 shows how the power factor of the supply varies with this simulated loading. It is observed that the power factor decreases from a value of 0.94 down to a poor 0.55 for the lowest DC motor load. The Figure also shows that the power factor for the same loading scenario with current compensation shows a large improvement achieving 0.975±0.01 across the whole operating scenario.

Figure 9 shows the AC supply current and voltage waveforms with the active filter in operation. It shows that changing the firing angle in the DC drive converter with varying load as in Figure 7 now has little effect on the relative position of the current, and the current waveform is much more sinusoidal. Measuring the total harmonic distortion (THD) of the current waveforms for a 30° firing angle shows that the active filter leads to a reduction from 9.99% down to 3.24%.

If the active filter is ideal then on average no real power should be drawn from the battery as the oscillating real term (9) has an average value of zero, and the reactive power compensation (10) does not affect the real power drawn by the battery. However as a result of the implementation of the active filter control scheme it was found that the average power is negative, which means that the battery is absorbing power, as shown in Figure 10. A real monitoring system has a finite bandwidth and response, and the inverter in the battery-inverter system has a limited switching frequency. Both reduce the accuracy of the compensation and real power can be unexpectedly drawn or absorbed by the battery. This can be easily compensated for by the battery state-of-charge controller.

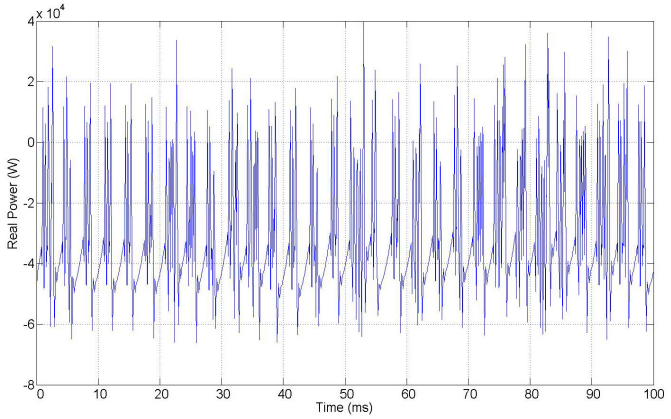


Fig. 10. Power Drawn From Battery

## V. Discussion

The simulation results provided illustrate the additional benefit the VTB simulation model brings to the design process. The original multiobjective optimisation assumes that the active filter mechanism is working ideally and that no power is being absorbed or drawn from the battery. Even if the active filter was working perfectly and the average battery power is zero, in the transient time domain the battery is varying from absorbing power to providing it. If the simulation battery model is extended to include a thermal model based upon the power demands on the battery like that of Figure 10, then the heating of the battery can be considered. This information will allow the designer to adapt the design either by adjusting the size or type of battery used, or provide an indication of the specification of cooling equipment required. The ability to drop in and out of the detailed simulation to check the results of the optimisation, and the tools to view the results, allow the designer freedom to choose properly between otherwise pareto optimal designs.

## VI. Conclusion

In this paper, a simulation model of the power and propulsion system of the James Clark Ross has been developed incorporating the dynamic behaviour of a propeller, DC motor, DC drive, battery and IGBT inverter covering electrical, mechanical and thermodynamic disciplines. The simulation is able to model transient behaviour, such as harmonics, that cannot be included in the steady state model used in the multiobjective optimisation process.

The MATLAB tool developed allows for the observation and exportation of potential optimal designs from a multiobjective design process. It offers an easy to use way of interpreting the sometimes confusing optimisation results allowing for the viewing of both design and objective variables in 2D, 3D and parallel coordinates.

## References

[1] A. Kallah, "Power and Propulsion Systems for the RRS James Clark Ross," Cegelec Projects.

[2] C. Fonseca and P. Fleming, "An overview of evolutionary algorithms in multiobjective optimization," *Evolutionary computation*, vol. 3, no. 1, pp. 1–16, 1995.

[3] P. Fleming, R. Purshouse, and R. Lygoe, "Many-objective optimization: An engineering design perspective," in *Evolutionary Multi-Criterion Optimization*. Springer, 2005, pp. 14–32.

[4] A. Molina-Cristobal, C. Papageorgiou, G. Parks, M. Smith, and P. Clarkson, "Multi-objective controller design: evolutionary algorithms and bilinear matrix inequalities for a passive suspension," *International Journal of Tomography and Statistics*, vol. 7, no. F07, pp. 31–36, 2007.

[5] J. Wu, N. Schulz, and W. Gao, "Distributed simulation for power system analysis including shipboard systems," *Electric Power Systems Research*, vol. 77, no. 8, pp. 1124–1131, 2007.

[6] R. Dougal, S. Liu, L. Gao, and M. Blackwelder, "Virtual test bed for advanced power sources," *Journal of Power Sources*, vol. 110, no. 2, pp. 285–294, 2002.

[7] H. Akagi, E. Watanabe, and M. Aredes, *Instantaneous power theory and applications to power conditioning*. Wiley-IEEE Press, 2007.

[8] E. Clarke, *Circuit analysis of AC power systems,Vol. 1 - symmetrical and related components*. J. Wiley & sons, inc., 1943.